Chromatography **2015**, *2*, 529-544; doi:10.3390/chromatography2030529

OPEN ACCESS

chromatography

ISSN 2227-9075

www.mdpi.com/journal/chromatography

Article

The Dramatic Modulatory Role of the 2'N Substitution of the Terminal Amino Hexose of Globotetraosylceramide in Determining Binding by Members of the Verotoxin Family

Murugesapillai Mylvaganam [1], Beth Binnington [1], Monique Budani [1,2], Anna M. Soltyk [3] and Clifford A. Lingwood [1,2,4,*]

[1] Program in Molecular Structure and Function, Research Institute, Peter Gilgan Centre for Research and Learning, The Hospital for Sick Children, 686 Bay Street, Toronto, Ontario M5G 0A4, Canada

[2] Laboratory Medicine & Pathobiology, University of Toronto, Toronto M5S 1A8, Canada

[3] Department of Cell and Systems Biology, University of Toronto Mississauga, Mississauga, ON L5L 1C6, Canada

[4] Department of Biochemistry, University of Toronto, Toronto, M5S 1A8, Canada

* Author to whom correspondence should be addressed; E-Mail: cling@sickkids.ca.

Academic Editor: Mark Devlin Maloney

Received: 27 April 2015 / Accepted: July 2015 / Published: 14 August 2015

Abstract: Although globotetraosylceramide (Gb_4) is only recognized by a single member of the verotoxin family namely, the pig edema disease toxin (VT2e), removal of the acetyl group from the terminal N-acetyl hexosamine of Gb_4 to generate the free amino sugar containing species (aminoGb4) results in the generation of a glycolipid preferentially recognized by all members of the verotoxin family (*i.e.*, VT1, VT2, VT2c, and VT2e). GT3, a site-specific mutant of VT2e, in which Gb_4 recognition is lost but Gb_3 binding is retained, also binds aminoGb4. We have now compared the binding of VT1, VT2, VT2e, and GT3 to a series of aminoGb4 derivatives using a TLC overlay technique. DimethylaminoGb4 is bound by VT1 and VT2 but not VT2e or GT3; formylaminoGb4 binds all toxins but poorly to VT2 and preferentially VT2e; trifluoroacetylaminoGb4 binds only VT2e and GT3; isopropylaminoGb4 binds VT1 and poorly to VT2; benzylaminoGb4 binds all four toxins. Thus, there is a marked distinction between the permissible amino substitutions for VT1 and VT2e binding. GT3 is a hybrid between these in that, according to the substitution, it behaves similarly either to VT1 or to VT2e. For each species, GT3 does not however, show a hybrid binding between that of VT1 and VT2e. Analysis of the binding as a function of pH shows

opposite effects for VT1 and VT2e: decreased pH increases VT1, but decreases VT2e receptor glycolipid binding.

Keywords: shiga toxin receptor; globotetraosylceramide; amino substitution

1. Introduction

Verotoxins (Shiga toxins) are a family of *E. coli* elaborated subunit toxins involved in microvascular disease [1,2]. VT1, VT2, and VT2c are produced by *E. coli* strains which colonize and affect humans, particularly children, whereas, VT2e is found in strains which infect pigs and is the cause of pig edema disease [3]. The pentameric B subunit of these toxins bind to a glycolipid receptor, globotriaosylceramide (galα1-4-galβ1-4 glucosylceramide, Gb_3) [4]. VT2e, however, binds to globotetraosylceramide (galNAcβ1-3galα1-4-galβ1-4glucosylceramide, Gb_4), the next homologue in the globo series of glycolipids, in addition to Gb_3 [5]. Although homologous, antibodies against VT1 or toxins of the VT2 series do not cross-neutralize cytotoxicity [6]. VT1 and VT2 are approximately 60% identical, whereas VT2 and VT2e are approximately 84% identical. Site specific mutagenesis of amino acids within the B subunit of VT2e (binds Gb_3 + Gb_4) to the corresponding amino acid found in VT2 (binds Gb_3 only), identified a double mutant (Gln64Glu/Lys66Gln,) termed GT3, in which the binding of Gb_4 was lost but that of Gb_3 retained [7]. This mutant showed an *in vivo* pathology which was similar to that of VT1 (Gb_3 binding-mediated) rather than that of VT2e [8].

Molecular modeling, in combination with an analysis of the binding of these toxins to deoxyGb_3 analogues resulted in the identification of two potential Gb_3 binding sites per B subunit monomer [9]. One site (cleft site or site 1) was between adjacent B subunit monomers while the other was in a shallow depression on the B subunit pentamer surface which opposes the plasma membrane of the target cell (site 2). By homology modeling, the binding of Gb_4 by VT2e and the lack of Gb_4 binding by GT3, were explained in terms of binding within the cleft site. The lack of binding of Gb_4 by the other verotoxins was consistent with binding in this site. In particular, the N-acetyl group of the terminal N-acetylgalactyosamine (galNAc) sugar of Gb_4 was identified as a primary basis for the lack of Gb_4 binding. An intramolecular H-bond from the 3OH of the galNAc to the acetyl oxygen prevented any reorientation of the NAc group to allow Gb_4 binding. Chemical removal of the N-acetyl moiety [10] to give the free amino sugar containing GSL, resulted in a species (aminoGb_4) which was highly effectively recognized by all members of the verotoxin family [9]. Docking of aminoGb_4 within the cleft site of VT1 demonstrated a salt bridge between the ammonium cation and the carboxylate anion of asparagine 16. The formation of such a stable linkage between the receptor and ligand provided a basis for the surprising observation of aminoGb_4 binding by all verotoxins and provided support for cleft site Gb_3 binding.

The co-crystal structure of the VT1 B subunit and a lipid-free Gb_3 oligosaccharide analogue was solved [11]. While the receptor density was found to correspond to the sites identified by modeling, the relative orientation of the sugar sequence within the binding sites, particularly site 2, were different from that modeled. In addition, density was associated with Trp34 (site 3). The structure of a similar VT1 complex was solved by NMR [12] which confirmed the preferential occupancy and sugar orientation of site 2 as in the crystal structure. Mutational studies provided evidence for the importance of all three

sites [13] but discrepancies between lipid-free sugar binding and cytotoxicity were evident [14]. Various globotriaose multimers binding in site 2, have proven effective in blocking cytotoxicity *in vitro* and *in vivo* [15–17]. The import of site 3 remains less well established [18,19]. This site is obstructed by the A subunit C terminus in VT2 [20] and empty in Gb_3 sugar co-crystals [21]. Similarly, this site was empty in the GT3/Gb_3 sugar co-crystal [22] but was proposed as a potential secondary Gb_4 binding site. Site 1 was partially occupied while site 2 was fully occupied in the co-crystal. The question of which site(s) bind membrane Gb_3 glycolipid may relate to the conformational differences of the GSL sugar relative to the membrane [23,24]. This is strongly influenced by the membrane cholesterol content [25], promoting a parallel conformation along the membrane surface, rather than a perpendicular orientation in which the carbohydrate protrudes from the membrane [26,27]. Such distinct Gb_3 conformers may bind in site 2 and site 1 respectively [28] as proposed [9].

Substitution/deletion of key residues in sites 1, 2, and 3 have shown all three sites to be important [13]. Gb_3 sugar binding only requires site 2, but membrane Gb_3 glycolipid binding requires all sites [14]. Recent studies show amino substitution within the terminal αgalactose of Gb_3 can enhance VT2 binding [29,30], although such structures are not made by mammalian cells. The X-ray structure of VT2 [20] and the co-crystal structure with such an "aminoGb_3" disaccharide derivative [21] supports binding in both sites 1 and 2.

Evidence indicates that the lipid moiety of membrane Gb_3 has a major impact on the recognition of the Gb_3 carbohydrate by the verotoxin B-subunit [24,31,32]. Lipid-free oligosaccharides may represent an inadequate model of verotoxin/membrane Gb_3 binding under physiological conditions. We now present evidence on the discriminatory binding of aminoGb_4 derivatives consistent with site 1 occupancy.

2. Materials and Methods

2.1. Materials

Solvents—dichloromethane (DCM), methanol (M), chloroform (C), acetonitrile (CH_3CN) and acetone (A)—were purchased from either Caledon (Georgetown, ON, Canada) or Aldrich (Milwaukee, WI, USA). Reagents were purchased from the following suppliers: Caledon—trifluoroacetic anhydride (TFA anhydride), triethylamine (Et_3N); Aldrich—37% aqueous formalin solution, N-hydroxysuccinimide (NHS); BDH (Toronto, ON, Canada)—30% H_2O_2; Sigma (St Louis, MO, USA)—4-chloro-1-naphthol, 1-ethyl-3-(3-dimethylaminopropyl)carbodiimide (EDAC), formic acid (99%), formic anhydride, sodium cyanoborohydride, 1-hydroxy-7-azabenzotriazole (HOAT); Fisher Scientific (Unionville, ON, Canada)—*para*-dimethylaminobenzaldehyde (NHBz-*p*NMe_2) and from BIO-RAD (Hercules, CA, USA)—goat anti-mouse and rabbit IgG horse radish peroxidase conjugate (GAM or GAR, respectively). Chromatographic materials—Silica gel, plastic backed TLC, (SilG, Machery & Nagel) and aluminum backed nanosilica plates (alugram NanoSIL GI UV_{254}, Macherey & Nagel)—were supplied by Caledon. Reverse phase C-18 cartridges were obtained from Waters (Mississauga, ON, Canada) and molecular sieves, 4 Å from Fisher.

Solvents were dried by storing over activated (~120 °C for 16 h) molecular sieves. Gb_3 and Gb_4 (or Gb_4•$NHCOCH_3$) were purified from human kidney as described [33]. Amino globoside (Gb_4•NH_2) was prepared by reaction of Gb_4 in 1 M $NaOH_{(aq)}$ at 102 °C for 3 h as described [10]. Chloroform was

dried by passing through an alumina column (Alumina:C; 1:5, v/v). Ammonical methanol was prepared by diluting 2 M NH_3 stock solution in EtOH with MeOH.

2.2. Methods

2.2.1. Synthesis of NMe_2, NHisoPr, or NHBz derivatives of Gb_4•NH_2

To a solution of Gb_4•NH_2 (2 mg, approximately 2 μmol) in dry chloroform (1 mL) were added approximately 3 equivalents (6 μmol) of the carbonyl reagent (formaldehyde, acetone, or PhCHO) and solid $NaCNBH_3$ (6 mg, 0.1 mmol). After stirring the reaction mixture for 16 h at room temperature (25 °C), chloroform was removed under a stream of N_2 and the remaining solid was then dissolved, by sonication, in 5 mL of distilled water. The resulting suspension was passed through a C-18 reverse phase cartridge, washed with 20 mL of water and eluted with 20 mL of ammonical methanol (0.2 M NH_3). Reaction products were further purified by silica gel column (2 × 2 cm) chromatography using C:M:H_2O; 60:30:2. Yields by TLC were greater than 85%.

2.2.2. Synthesis of Gb_4•$NHCOCF_3$

Acylating reagent trifluoroacetyl imidazole was prepared by adding a DCM solution of the anhydride ($(F_3CCO)_2O$, 0.85 g, 2.7 mmol) divided in 3 portions (1 mL) at 15 min intervals to an imidazole (0.41 g, 6.0 mmol) suspension in DCM (3 mL). The reaction mixture was stirred for 2 h and was assumed to be approximately a 0.5 M solution of the imidazole derivative.

A solution (20 μL, 10 μmol) of the imidazole derivative was added to a solution of Gb_4•NH_2 (1 mg) in methanol (1 mL) and the reaction was monitored by TLC (C:M:H_2O^S; 60:35:8). Appearance of many orcinol positive products suggests some degree of acylation of OH groups. Once all the Gb_4•NH_2 was consumed, ammonia (0.1 mL of 2 M NH_3 in EtOH) was added and the mixture was dried under a stream of N_2. If a significant degree of O-acylation had occurred, the dried residue was treated with a solution of Et_3N:M:H_2O; 2:6:10 (0.5 mL/mg of GSL) at room temperature and monitored by TLC (C:M:H_2O^{Salt}; 60:35:8 −0.25% KCl). Once the O-acyl group hydrolysis was complete the material was dried under a stream of N_2, and purified on a silica gel column (0.5 × 2 cm) using C:M:H_2O; 60:30:2. Yield 75%.

2.2.3. Synthesis of Gb_4•NHCOH

To a solution (1 mL of 5:1, CH_3CN:Et_3N) of Gb_4•NH_2 (0.5 mg) was added the following reagents in the given order; formic acid (30 μL), HOAT (1.5 equivalents) and EDAC (3 equivalents). The mixture was stirred for 18 h at 60 °C and dried under a stream of N_2. Crude product was purified on a silica gel column using C:M:H_2O; 60:30:2. Yield, ~60%, rest was Gb_4•NH_2.

2.2.4. Mass Spectroscopic Analyses

Pure samples were dissolved in 9:1, M:H_2O mixture containing 0.1% NaCl and the ES spectra were recorded on a SCIEX API III spectrometer. The acyl derivatives, natural Gb_4 which has a terminal N-acetyl galactosamine or the corresponding formyl group of the trifluoro acetyl analogues predominantly give the sodium adduct. However the aminoGb_4 and its alkylated derivatives predominantly gave the proton adduct.

TLC Overlay

Toxins were purified as previously described [34]. The site-specific mutants were previously described [14]. Toxin binding to GSLs was assayed by TLC overlay as previously described [35]. GSL-bound VT1 and the VT1 B-subunit mutants were detected with mAb PH1 while VT2e, GT3, and VT2 were visualized using rabbit anti-VT2e [8] (a generous gift of Dr. Carlton Gyles, University of Guelph).

Receptor ELISA (RELISA)

Glycolipids were coated on microtitre plate wells by evaporation from ethanolic solution. GSL aliquots were measured from stock solutions in dichloromethane/methanol (2:1, v/v) into screw-capped glass tubes, and the solvent was removed under a stream of nitrogen. Ethanol was added to the lipid residue, and a uniform glycolipid solution was prepared by immersing the tube for 30 s in a bath sonicator followed by 1 min of vortexing. A 100 µL aliquot of ethanolic GSL (0.5 µg/mL) was added per well in triplicate and the ethanol was allowed to evaporate at room temperature overnight. Once dry, the plates were stored in a desiccator at 4 °C. Wells were blocked with 200 µL of 0.2% (w/v) BSA in 10 mM sodium phosphate/150 mM NaCl, pH 7.4 (BSA-PBS) for 1–2 h, then the wells were washed twice with 150 µL/well 0.2% BSA-PBS. The following incubations were carried out in BSA-PBS at room temperature for 1 h. VT (200 ng/mL), primary antibody (mouse anti-VT1 mAb PH1, 1 µg/mL or rabbit anti-VT2e, 1/2000), goat anti-mouse or rabbit IgG-HRP conjugate (1/2000). Between incubations, wells were washed three times with 200 µL of 0.2% BSA-PBS. Finally wells were incubated with substrate solution, 0.5 mg/mL 2,2'-azino-bis-(3-ethylbenzthiazoline-6-sulphonic) diammonium salt (ABTS), 0.01% H_2O_2 in 0.08 M citric acid/0.1 M disodium phosphate, pH 4.0. After sufficient color had developed (usually 10–20 min), the absorbance of each well at 405 nm was measured using an ELISA plate reader.

3. Results

The structures of the aminoGb$_4$ derivatives studied are shown in Figure 1. Mass spectrometry confirmed the structures of formylaminoGb$_4$, TFAaminoGb$_4$, and dimethyl-aminoGb$_4$ (Tables 1 and 2). The isopropyl and benzyl species were found to be monosubstituted (Table 2).

TLC overlay assay of the binding of VT1, VT2e, GT3, and VT2 are shown in Figure 2. A distinct pattern of recognition of the aminoGb$_4$ derivatives is seen for each toxin. As expected, Gb$_4$ was bound only by VT2e, and aminoGb$_4$ and Gb$_3$ were bound equally by all toxins, except VT2 which preferentially bound aminoGb$_4$. DimethylaminoGb$_4$ and isopropylaminoGb$_4$ were bound only by VT1 and VT2 but VT2 bound significantly less isopropylaminoGb$_4$. FormylaminoGb$_4$ bound all four toxins, but poorly to VT2 and preferentially VT2e, while benzylaminoGb$_4$ bound all four toxins equally. TFAaminoGb$_4$ was strongly bound by VT2e and GT3 but not at all by VT1 or VT2. The aminoGb$_4$ derivative binding is thus divided into two groups: VT1/VT2 (bind dimethyl and isopropyl) and VT2e/GT3 (bind TFA but not dimethyl or isopropyl). VT1 and VT2 are distinguished by the reduced binding of VT2 to Gb$_3$ and isopropylaminoGb$_4$, while VT2e and GT3 are distinguished by the Gb$_4$ and increased formylaminoGb$_4$ binding of VT2e (Table 3).

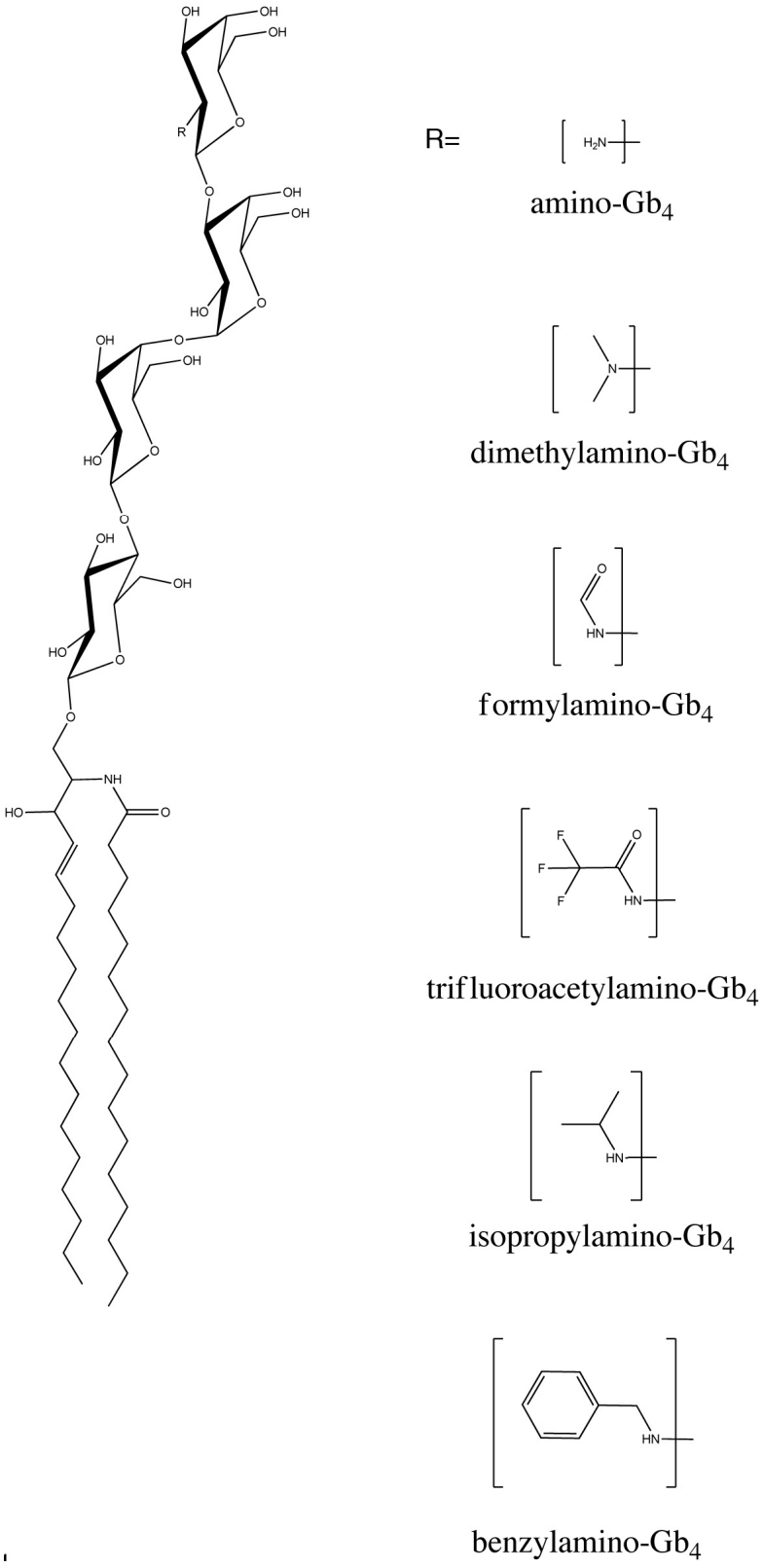

Figure 1. Structure of aminoGb4 derivatives.

Table 1. Tabulation of major subspecies (*i.e.*, having different acyl chains) of Gb_4 and Gb_4-acyl derivatives and their corresponding molecular ions determined by mass spectrometry. ND not detected. N = acyl chain carbon number. Gb_4 = globotetraosylceramide.

n	Gb_4•NHCOCH$_3$		Gb_4•NHCOH		Gb_4•NHCOCF$_3$	
	M+H (%)	M+Na (%)	M+H (%)	M+Na (%)	M+H (%)	M+Na (%)
22	1312.0 (30)	1334.0 (74)	ND	1320.0 (7)	ND	1388.0 (36)
24	1340.0 (39)	1362.2 (100)	ND	1348.0 (15)	ND	1416.2 (43)
24:1	ND	1360.0 (78)	ND	1346.0 (8)	ND	1414.2 (29)

Table 2. Major subspecies (*i.e.*, having different acyl chains) of amino Gb_4 derivatives and their corresponding molecular ions.

n	Gb_4•NH$_2$	Gb_4•NMe$_2$	Gb_4•NHBz-*p*NMe$_2$	Gb_4•NHisoPr
	M+H (%)	M+H (%)	M+H (%)	M+H (%)
22	1270.2 (8)	1298.2 (<2)	1403.0 (32)	1340.2 (98)
24	1298.0 (16)	1326.2 (<2)	1431.0 (39)	1338.2 (100)
24:1	1296.0 (11)	1324.2 (<2)	1429.2 (38)	1312.0 (65)

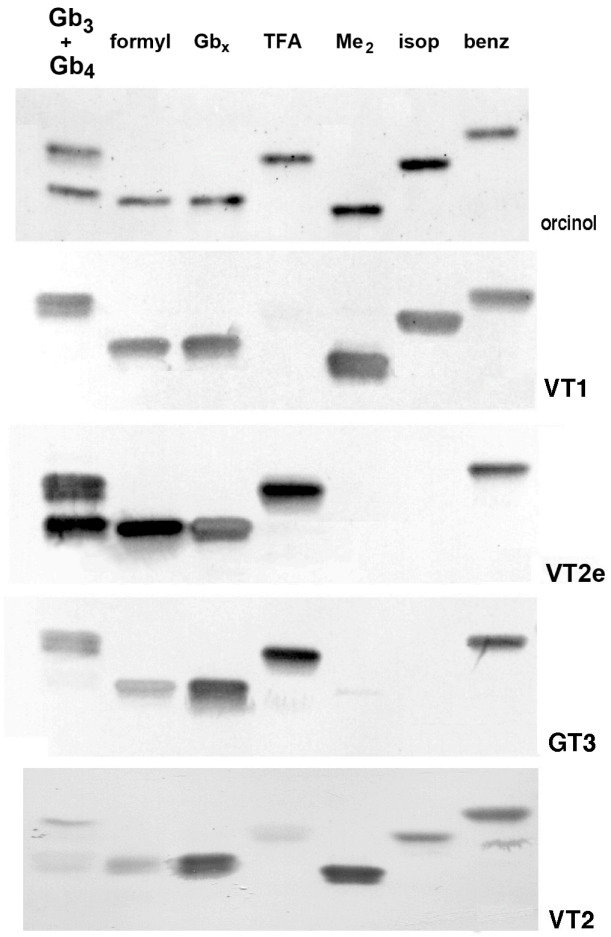

Figure 2. Comparison of the binding of VT1, VT2e, GT3, and VT2 binding by TLC overlay to lane 1–Gb_3 + Gb_4, lane 2–formyl-aminoGb_4, lane 3–aminoGb_4, lane 4–TFAaminoGb_4, lane 5–dimethylaminoGb_4, lane 6–isopropylaminoGb_4, lane 7–benzylaminoGb_4. Species detected by orcinol spray are shown in upper panel.

Table 3. Summary of GSL binding.

GSL	VT1	VT2	VT2e	GT3
Gb_3	+	+	+	+
Formyl$aminoGb_4$	+	+	+	+
Gb_4	-	-	+	-
TFA$aminoGb_4$	-	-	+	+
Dimethyl$aminoGb_4$	+	+	-	-
isopropyl$aminoGb_4$	+	+	-	-
Benzyl$aminoGb_4$	+	+	+	+

Effect of pH. The binding of VT2e and VT1 were then compared at different pHs. Glycolipid receptor binding was assayed by TLC overlay at pH 9.0, 6.0, and 4.5 (Figure 3A). For VT1, all species tested, Gb_3, aminoGb_4, dimethylaminoGb_4, isopropylaminoGb_4 and benzylaminoGb_4 were less strongly bound at high pH. In contrast, VT2e binding to these aminoGb_4 derivatives was reduced at low pH. Gb_3, Gb_4, and aminoGb_4 were strongly bound by VT2e at pH 9.0. Significant VT2e binding to benzylaminoGb_4 was seen but dimethylaminoGb_4 and isopropylaminoGb_4 were not recognized at any pH. Binding to Gb_3, Gb_4, and aminoGb_4 and benzylaminoGb_4 was reduced at pH 6.0 and further at pH 4.5. The effect of pH on aminoGb_4 derivative binding by VT1, VT2e, and GT3 was also assayed by RELISA (Figure 3B). Consistent with TLC binding, the dimethyl and isopropyl species were only significantly bound by VT1. VT1 binding Gb_4, not detected by TLC overlay, was however, significant by RELISA and remarkably, acid pH dependent, being greatly reduced at physiological pH, and eliminated at high pH. Gb_4 RELISA binding was also pH sensitive for GT3, but not VT2e. VT1 and GT3 Gb_3 binding were also reduced at increased pH. At physiological pH, a four-fold preference for Gb_3 over Gb_4 was maintained for VT1 but GT3 Gb_3/Gb_4 binding was equivalent. Of the aminoGb_4 derivatives, only TFA-aminoGb_4/VT1 binding was reduced at high pH. TFA$aminoGb_4$ binding was not pH sensitive for VT2e or GT3. VT2e binding benzylaminoGb_4 was reduced at low pH (as seen by TLC-Figure 3A). AminoGb_4/VT2e binding was reduced at low pH but recognition of other species, notably Gb_3 and Gb_4 was unaffected. Only VT2e bound the pentahexoside Forssman glycolipid. This binding has not been previously reported. GT3 showed pH dependent Gb_3 and Gb_4 binding (similar to VT1), but did not bind dimethyl or isopropylaminoGb_4 (similar to VT2e). Binding to the control GSLs, gangliotriaosylceramide (Gg_3) and lactosylceramide (LacCer) was not seen at any pH, ruling out non-specific interactions induced by high or low pH treatment of the toxins.

Site specific mutants. Several site-specific VT1 mutants (and double mutants), in which a key amino acid within one of the three proposed receptor binding sites was deleted, were assessed for binding the aminoGb_4 species by TLC overlay (Figure 4). Phe30 is a key residue in site 1 and, to a lesser extent, site 2 [14]. Its mutation to alanine resulted in the loss of Gb_3 and Gb_4, TFA$aminoGb_4$, and aminoGb_4 binding (In this experiment, the formylaminoGb_4 sample contained a trace of unreacted aminoGb_4, below the limit of detection by orcinol but bound by wildtype VT1). Phe30Ala retains residual binding to dimethyl, isopropyl and benzyl- aminoGb_4. This was consistent with RELISA (Figure 5) which showed similar loss of Gb_3, aminoGb_4 and formylaminoGb_4 binding while dimethyl- and benzyl-aminoGb_4 binding were retained. Glycine 62 is in site 2. For this mutant, binding to all species was deleted (Figure 4). However, in the combination double mutant, binding to dimethyl-, isopropyl- and benzyl-aminoGb_4 was prevented and binding was similar to Phe30Ala. The loss of Alanine 56, also an important

residue in site 2, showed a milder phenotype in which binding to all aminoGb$_4$ derivatives, except TFA and formyl species, was retained. Asp 17 is key in site 1 [14]. Mutation to glutamic acid deleted Gb$_3$ and TFA and formyl-aminoGb$_4$ recognition but dimethyl-, isopropyl- and benzyl-aminoGb$_4$ binding were fully retained. Deletion of site 3 by mutation of tryptophan 34 which lines the B pentamer central pore [11] resulted in the loss of all binding. This phenotype was retained when combined with Asp17Glu.

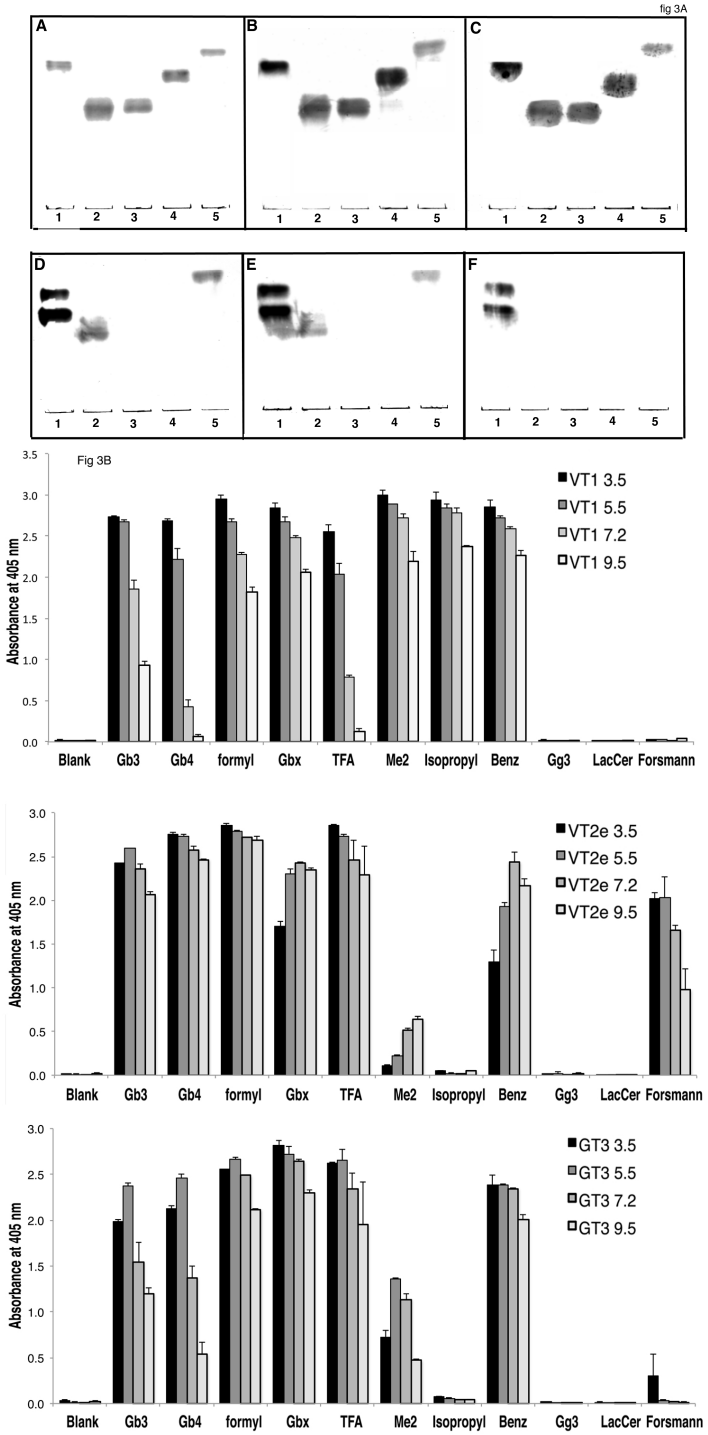

Figure 3. Effect of pH 9.0 (**A**,**D**), pH 6.0 (**B**,**E**), and pH 4.5 (**C**,**F**) on the binding of VT1 (A,B,C) and VT2e (D,E,F) to lane 1–Gb$_3$ + Gb$_4$, lane 2–aminoGb$_4$, lane 3–dimethylaminoGb$_4$, lane 4–isopropylaminoGb$_4$, lane 5–benzylaminoGb$_4$, monitored by TLC overlay (A) and receptor ELISA (B).

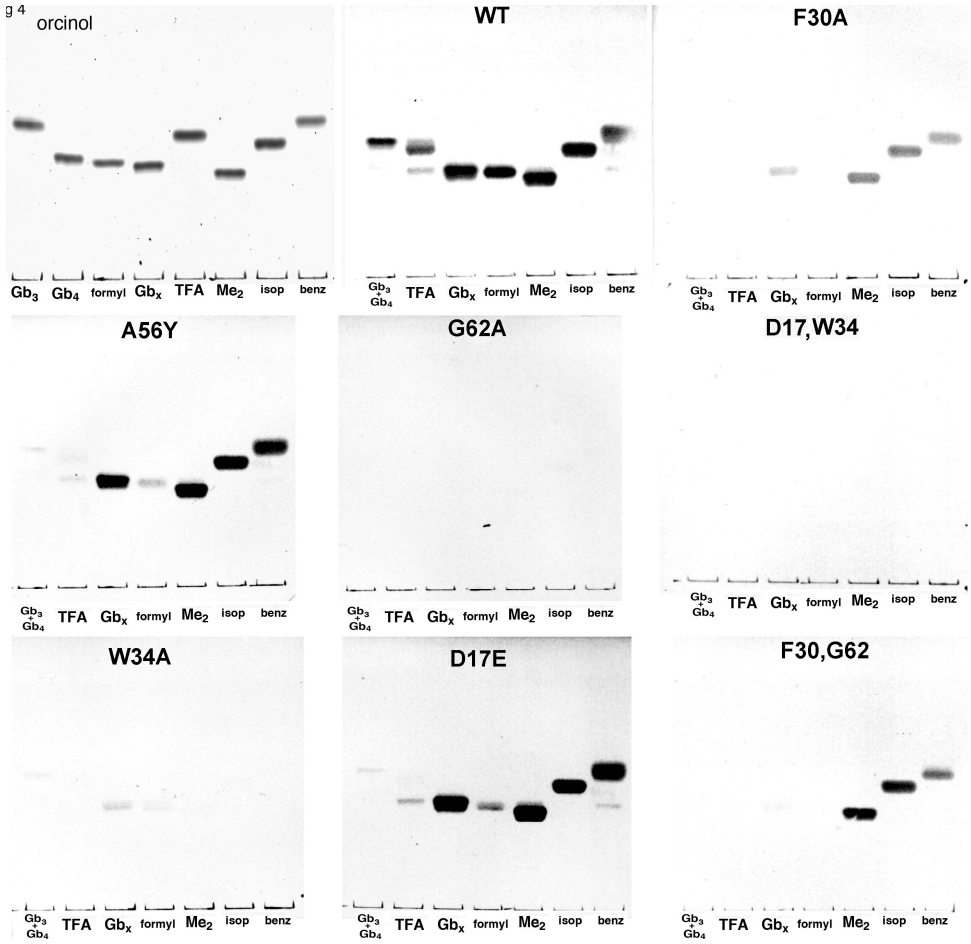

Figure 4. Binding of VT1 mutants to aminoGb4 derivatives. The aminoGb4 derivatives were separated by TLC and chemically stained for carbohydrate with orcinol. The binding of these derivatives to wildtype VT1 was compared to that of the site deletion mutants Phe30Ala (site 1), Ala56Tyr (site 2), Gly62Ala (site 2), Trp34Ala (site 3), Arg17Glu (site 1), and the double mutant Phe30Ala/Gly62Ala by TLC overlay.

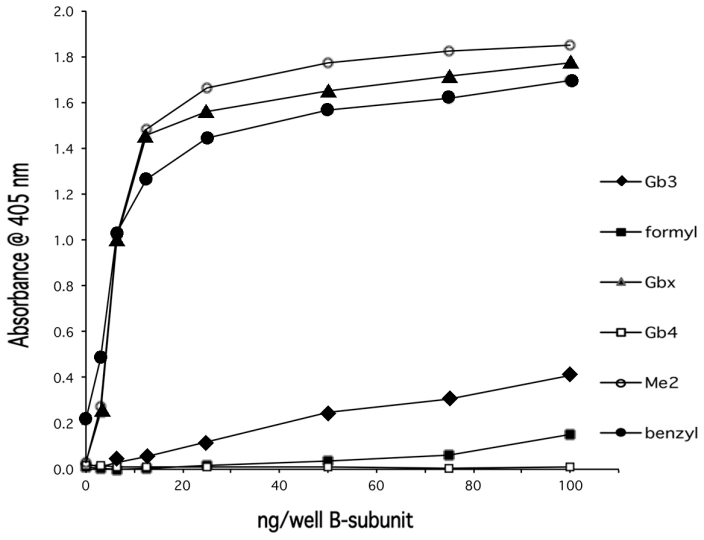

Figure 5. Phe30Ala VT1 B mutant retains recognition of an aminoGb4 derivative subset. Dose response RELISA shows while binding of F30A VT1 B-subunit to Gb3 is minimal, binding to aminoGb4 derivatives, except formylaminoGb4, is retained.

4. Discussion

Following the original discovery that VT2e, unlike the other members of the verotoxin family, can bind to Gb_4 in addition to Gb_3 [5], it was assumed it is the presence of the additional terminal sugar which prevents VT1, VT2 ,and VT2c from binding Gb_4. Our observation that aminoGb4 is preferentially recognized by VT1, VT2, and VT2c, even compared with Gb_3 [9], demonstrated this is not the case. Thus the cleft site of all verotoxins can accommodate a four sugar containing globo-series glycolipid.

We consistently observe a lack of VT1 or VT2 binding to Gb_4 by TLC overlay, but other studies have reported a weaker receptor function for Gb_4 [32,36,37]. The current and previous studies show that VT1 binding to solid phase Gb_4 can be induced under some conditions [38]. We have also anecdotally found that 'old' toxin begins to show some Gb_4 recognition. This could be interpreted as increased accommodation by the subunit cleft site (site1) due to some degree of pentamer long-term instability [39].

The basis for the lack of Gb_4 binding by VT1, VT2, and VT2c is therefore subtle. In our early molecular modeling studies, we proposed that the pocket between the side chains of Asp16 and Asp17 in VT1 was not sufficient to accommodate the acetamido group of Gb_4 and that the unfavorable orientation of the carboxyl group of the acetamido group towards the carboxyl group of Asp16 would prevent Gb_4 binding. The N-acetyl group cannot reorient to accommodate this unfavorable interaction because of an intramolecular hydrogen bond from the 3' hydroxyl of the GalNAc residue to the carbonyl oxygen of the N-acetyl group [9]. In VT2e, a pocket between Asp16 and Glu15 accommodates the acetamido group of the terminal GalNAc of Gb_4 to allow binding. The NAc group does not stabilize the interaction in any way. The TFA derivative is larger than the NAc group and on this basis, should only bind VT2e and GT3 as observed.

The pH dependency of VT1 binding is consistent with an important role for the charge on the nitrogen of the aminohexose for binding, presumably in the formation of a salt bridge with the carboxyl group of Asp16 [9]. The lack of VT1 recognition of TFAaminoGb4 and reduced recognition of formylaminoGb4 is consistent with the repulsion of the carbonyl oxygen of the acetyl group of the aminohexose of Gb_4 by the carboxyl group of Asp16 as proposed to explain the lack of VT1/Gb_4 binding [9]. In formylaminoGb4, although the carbonyl oxygen will be restricted in the same way as in Gb_4, the volume of the proton (of the formyl group) as opposed to the methyl group (of the acetyl group) will be less. This may allow some access to the trough between Asp17-16 side chains [9] to explain the low but significant VT1/formylaminoGb4 binding. Once this oxygen is removed, as in isopropylaminoGb4 and dimethylaminoGb4, binding to VT1 is allowed. From our published model [9], the amine of aminoGb4 in site 1 is directed towards solvent. Thus, when the constraint of the carbonyl oxygen is removed, there should be little size restriction for the amino substituent to retain binding. This would explain the isopropylaminoGb4/VT1 binding.

The current data indicates that the binding of aminoGb4 by VT2e does not involve the formation of a salt bridge. In contrast to VT1, the receptor binding of VT2e is reduced at lower pH. AminoGb4 is not bound by VT2e at pH4.5. This is not consistent with the involvement of a salt bridge in VT2e/aminoGb4 recognition. In VT2e, the trough between Asp16 and Glu15 is larger than that between Asp17 and Asp16 in VT1 and can accommodate the NAc group of Gb_4 [9]. Similarly, this trough could accommodate the TFA and formyl groups to explain the VT2e binding of TFAaminoGb4 and formylaminoGb4. The nitrogen of aminoGb4 docked in site I of VT2e is too far from the carboxyl group of Asp16, and may

also be too far from that of Glu15, to form a salt bridge [9]. Moreover, the region in VT2e corresponding to the 'Asp loop' of VT1 is less negatively charged and could be neutralized at acid pH. The absence of a salt bridge, could explain the pH dependency of VT2e binding. The VT2e B subunit has an overall charge of 2+ [40] which would disfavor aminoGb$_4$ binding, particularly at low pH. However, the lack of VT2e binding to dimethylaminoGb$_4$ and isopropylaminoGb$_4$ cannot be explained without detailed modeling of these complexes. In the absence of a salt bridge, the amine protons, missing in dimethylaminoGb$_4$, may be required for H-bonding to stabilize the VT2e complex, explaining the lack of VT2e recognition. It is also possible that this is a steric problem. Although we had planned to generate the dibenzylaminoGb$_4$ derivative, mass spectrometry showed mono substitution had occurred. Thus an amide proton is available to explain the VT2e binding. However the amide proton is also available in isopropylaminoGb$_4$ yet this is not bound by VT2e. The isopropyl group is considerably bulkier than the benzyl and this may account for the difference.

It is to some extent ironic that while VT2e is the only toxin to bind Gb$_4$, it is the only toxin which will not bind the dimethyl or isopropyl derivatives. Indeed all the species substituted with hydrophobic groups are poorly recognized by VT2e but effectively bound by VT1. Those substitutions of aminoGb$_4$ which have little effect on VT2e binding (formyl, TFA) remove VT1 recognition.

Our original model [9] explained the lack of binding of Gb$_4$ by the double mutant GT3 and the fact that the single mutation in VT2e of either Gln64Glu or Lys66Gln alone has no effect on Gb$_4$ binding. The modeling of Gb$_4$ binding to VT2e, based on the co-crystal structure of Gb$_3$ oligosaccharide in site 1 of VT1 [41], is consistent with the loss of Gb$_4$ binding by GT3 since the terminal galNAc interacts with both VT2e Lys66 and Gln64. However, this study proposes two H-bonds from Lys13 and Glu16 to the NAc carbonyl oxygen which would be lost in the case of aminoGb$_4$. Thus the binding of the lipid-free Gb$_3$ sugar in site 1 [11] as determined from the co-crystal, does not provide an explanation for the high affinity binding of aminoGb$_4$.

Modeling of GT3 with Gb$_3$ or aminoGb$_4$ was not performed and thus, an explanation for the binding specificity of GT3 must be speculative. Overall, the present results show receptor binding is more complex than previously envisioned. In terms of the importance of the carbonyl oxygen on the amide nitrogen, GT3 behaves as VT1 and does not bind formylaminoGb$_4$, consistent with our proposal that the trough between Asp16 and Glu15 is compromised in GT3 [9]. However GT3 does bind TFAaminoGb$_4$, unlike VT1, suggesting that this trough is distinct from that between Asp17 and Asp16 in VT1. Site 1 or site 2 modification blocks Gb$_3$, aminoGb$_4$, formylaminoGb$_4$ recognition with little effect on dimethyl- or isopropyl-aminoGb$_4$ binding, suggesting a different binding mechanism for these latter GSL analogues, likely related to the lack of binding of the latter group by VT2e and GT3. The resolution of such questions however, must await the crystal structure of GT3, VT2e and the modeling of their site 1 / 2 docked receptors.

In summary, we have documented a remarkable dependence on the amino substitution of aminoGb$_4$ in terms of variable binding to VT1, GT3, and VT2e, as well as a distinct pH dependency for VT1 as opposed to VT2e with regard to glycolipid receptor binding. For the most part, these differences are consistent with our previous modeling of aminoGb$_4$ binding in site 1 of the verotoxin B subunit pentamer.

Acknowledgements

This study was supported by CIHR grant #MT13073.

Author Contributions

Murugesapillai Mylvaganam synthesized and characterized the aminoGb4 derivatives; Beth Binnington performed the experiments and analyzed data, Monique Budani analyzed data and prepared the paper, Anna Soltyk prepared mutant toxins, Clifford Lingwood designed the experiments, analyzed data and wrote the paper.

Conflicts of Interest

The authors declare no conflict of interest.

Abbreviations

VT1, Verotoxin 1 (aka Shiga-like toxin1, Slt1, Shiga toxin1, Stx1), the prototype *E. coli* derived AB_5 subunit toxin with virtual identity to Shiga toxin from *S. dysenteriae*. Gb_3 is the functional receptor; VT2, Verotoxin 2 (Stx2), *E. coli* toxin B subunit is 66% homologous to VT1B, family member most associated with human disease. Gb_3 is the functional receptor; VT2e, Less toxic VT2 family member. B subunit 96% homologous to VT2. Gb_4 is the functional receptor; RELISA, receptor enzyme linked immunoassay; GSL, glycosphingolipid.

References

1. Bauwens, A.; Betz, J.; Meisen, I.; Kemper, B.; Karch, H.; Muthing, J. Facing glycosphingolipid-Shiga toxin interaction: Dire straits for endothelial cells of the human vasculature. *Cell. Mol. Life Sci.* **2012**, *70*, 452–457.
2. Page, A.V.; Liles, W.C. Enterohemorrhagic Escherichia coli Infections and the Hemolytic-Uremic Syndrome. *Med. Clin. N. Am.* **2013**, *97*, 681–695.
3. MacLeod, D.L.; Gyles, C.L.; Wilcock, B.P. Reproduction of Edema Disease of Swine with Purified Shiga-like Toxin-II Variant. *Vet. Pathol.* **1991**, *28*, 66–73.
4. Lingwood, C.A. Verotoxin recognition of its glycolipid receptor, globotriaosylceramide: Role in pathogenesis. In *Recent Advances in Verocytotoxin-Producing Escherichia Coli* Infections; Karmali, M.A., Goglio, A.G., Eds.; Elsevier Science B.V.: Bergamo, Italy, 1994; pp. 131–137.
5. DeGrandis, S.; Law, H.; Brunton, J.; Gyles, C.; Lingwood, C.A. Globotetraosyl ceramide is recognized by the pig edema disease toxin. *J. Biol. Chem.* **1989**, *264*, 12520–12525.
6. Head, S.; Karmali, M.; Lingwood, C.A. Preparation of VT1 and VT2 hybrid toxins from their purified dissociated subunits: Evidence for B subunit modulation of A subunit function. *J. Biol. Chem.* **1991**, *266*, 3617–3621.
7. Tyrrell, G.J.; Ramotar, K.; Toye, B.; Boyd, B.; Lingwood, C.A.; Brunton, J.L. Alteration of the carbohydrate binding specificity of verotoxins from Galα1-4Gal to GalNAc*β*1-3Galα1-4Gal and vice versa by site-directed mutagenesis of the binding subunit. *Proc. Natl. Acad. Sci. USA* **1992**, *89*, 524–528.

8. Boyd, B.; Tyrrell, G.; Maloney, M.; Gyles, C.; Brunton, J.; Lingwood, C. Alteration of the glycolipid binding specificity of the pig edema toxin from globotetraosyl to globotriaosyl ceramide alters *in vivo* tissue targetting and results in a VT1-like disease in pigs. *J. Exp. Med.* **1993**, *177*, 1745–1753.
9. Nyholm, P.G.; Magnusson, G.; Zheng, Z.; Norel, R.; Binnington-Boyd, B.; Lingwood, C.A. Two distinct binding sites for globotriaosyl ceramide on verotoxins: molecular modelling and confirmation by analogue studies and a new glycolipid receptor for all verotoxins. *Chem. Biol.* **1996**, *3*, 263–275.
10. Lingwood, C.A.; Nutikka, A. A novel chemical procedure for the selective removal of nonreducing terminal *N*-acetyl residues from glycolipids. *Anal. Biochem.* **1994**, *217*, 119–123.
11. Ling, H.; Boodhoo, A.; Hazes, B.; Cummings, M.; Armstrong, G.; Brunton, J.; Read, R.J. Structure of the Shiga toxin B-pentamer complexed with an analogue of its receptor Gb_3. *Biochemistry* **1998**, *37*, 1777–1788.
12. Richardson, J.M.; Evans, P.D.; Homans, S.W.; Donohue-Rolfe, A. Solution structure of the carbohydrate-binding B-subunit homopentamer of verotoxin VT-1 from *E. coli*. *Nat. Struct. Biol.* **1996**, *4*, 190–193.
13. Bast, D.J.; Banerjee, L.; Clark, C.; Read, R.J.; Brunton, J.L. The identification of three biologically relevant globotriaosyl ceramide receptor binding sites on the verotoxin 1 B subunit. *Mol. Microbiol.* **1999**, *32*, 953–960.
14. Soltyk, A.M.; MacKenzie, C.R.; Wolski, V.M.; Hirama, T.; Kitov, P.I.; Bundle, D.R.; Brunton, J. A mutational analysis of the Globotriaosylceramide binding sites of Verotoxin VT1. *J. Biol. Chem.* **2002**, *277*, 5351–5359.
15. Nishikawa, K.; Matsuoka, K.; Watanabe, M.; Igai, K.; Hino, K.; Hatano, K.; Yamada, A.; Abe, N.; Terunuma, D.; Kuzuhara, H.; *et al.* Identification of the optimal structure required for a shiga toxin neutralizer with oriented carbohydrates to function in the circulation. *J. Infect. Dis.* **2005**, *191*, 2097–2105.
16. Watanabe, M.; Igai, K.; Matsuoka, K.; Miyagawa, A.; Watanabe, T.; Yanoshita, R.; Samejima, Y.; Terunuma, D.; Natori, Y.; Nishikawa, K. Structural analysis of the interaction between Shiga toxin B subunits and linear polymers bearing clustered globotriose residues. *Infect. Immun.* **2006**, *74*, 1984–1988.
17. Kitov, P.I.; Mulvey, G.L.; Griener, T.P.; Lipinski, T.; Solomon, D.; Paszkiewicz, E.; Jacobson, J.; Sadowska, J.; Suzuki, M.; Yamamura, Y.; *et al. In viv*o supramolecular templating enhances the activity of multivalent ligands: a potential therapeutic against the Escherichia coli O157 AB5 toxins. *Proc. Natl. Acad. Sci. USA* **2008**, *105*, 16837–16842.
18. Shimizu, H.; Field, R.A.; Homans, S.W.; Donohue-Rolfe, A. Solution structure of the complex between the B-subunit homopentamer of verotoxin VT-1 from *Escherichia* coli and the trisaccharide moiety of globotriaosylceramide. *Biochemistry* **1998**, *37*, 11078–11082.
19. Thompson, G.; Shimizu, H.; Homans, S.; Donohue-Rolfe, A. Localization of the binding site for the oligosaccharide moiety of Gb3 on verotoxin 1 using NMR residual dipolar coupling measurements. *Biochemistry* **2000**, *39*, 13153–13156.

20. Fraser, M.E.; Fujinaga, M.; Cherney, M.M.; Melton-Celsa, A.R.; Twiddy, E.M.; O'Brien, A.D.; James, M.; Structure of shiga toxin type 2 (Stx2) from escherichia coli O157:H7. *J. Biol. Chem.* **2004**, *279*, 27511–27517.
21. Jacobson, J.M.; Yin, J.; Kitov, P.I.; Mulvey, G.; Griener, T.P.; James, M.N.; Armstrong, G.; Bundle, D. The crystal structure of shiga toxin type 2 with bound disaccharide guides the design of a heterobifunctional toxin inhibitor. *J. Biol. Chem.* **2014**, *289*, 885–894.
22. Ling, H.; Pannu, N.S.; Boodhoo, A.; Armstrong, G.D.; Clark, C.G.; Brunton, J.L.; Read, R. A mutant Shiga-like toxin IIe bound to its receptor Gb3: Structure of a group II Shiga-like toxin with altered binding specificity. *Structure* **2000**, *8*, 253–264.
23. Nyholm, P.-G.; Pascher, I. Orientation of the saccharide chains of glycolipids at the membrane surface: Conformational analysis of the glucose-ceramide and the glucose-glyceride linkages using molecular mechanics (MM3). *Biochemistry* **1993**, *32*, 1225–1234.
24. Watkins, E.B.; Gao, H.; Dennison, A.J.; Chopin, N.; Struth, B.; Arnold, T.; Florent, J.-C.; Johannes, L. Carbohydrate conformation and lipid condensation in monolayers containing glycosphingolipid Gb3: Influence of acyl chain structure. *Biophys. J.* **2014**, *107*, 1146–1155.
25. Mahfoud, R.; Manis, A.; Binnington, B.; Ackerley, C.; Lingwood, C.A. A major fraction of glycosphingolipids in model and cellular cholesterol containing membranes are undetectable by their binding proteins. *J. Biol. Chem.* **2010**, *285*, 36049–36059.
26. Yahi, N.; Aulas, A.; Fantini, J. How cholesterol constrains glycolipid conformation for optimal recognition of Alzheimer's beta amyloid peptide (Abeta1-40). *PLoS One* **2010**, *5*, e9079.
27. Lingwood, D.; Binnington, B.; Róg, T.; Vattulainen, I.; Grzybek, M.; Coskun, U.; Lingwood, C.; Simons, K. Cholesterol modulates glycolipid conformation and receptor activity. *Nat. Chem. Biol.* **2011**, *7*, 260–262.
28. Lingwood, C.A. Receptor-related Risk Factors for Verotoxin Pathogenesis. In *Bacterial Toxins - Genetics, Molecular Biology and Novel Applications*; Proft, T., Ed.; Caister Acedemic Press: Norfolk, UK, 2013; pp. 1–12.
29. Kale, R.R.; McGannon, C.M.; Fuller-Schaefer, C.; Hatch, D.M.; Flagler, M.J.; Gamage, S.D.; Weiss, A.; Iyer, S. Differentiation between structurally homologous Shiga 1 and Shiga 2 toxins by using synthetic glycoconjugates. *Angew. Chem. Int. Ed. Engl.* **2008**, *47*, 1265–1268.
30. Flagler, M.J.; Mahajan, S.S.; Kulkarni, A.A.; Iyer, S.S.; Weiss, A.A. Comparison of binding platforms yields insights into receptor binding differences between shiga toxins 1 and 2. *Biochemistry* **2010**, *49*, 1649–1657.
31. Kiarash, A.; Boyd, B.; Lingwood, C.A. Glycosphingolipid receptor function is modified by fatty acid content: Verotoxin 1 and Verotoxin 2c preferentially recognize different globotriaosyl ceramide fatty acid homologues. *J. Biol. Chem.* **1994**, *269*, 11138–11146.
32. Gallegos, K.M.; Conrady, D.G.; Karve, S.S.; Gunasekera, T.S.; Herr, A.B.; Weiss, A.A. Shiga toxin binding to glycolipids and glycans. *PLoS One* **2012**, *7*, e30368.
33. Boyd, B.; Lingwood, C.A. Verotoxin receptor glycolipid in human renal tissue. *Nephron* **1989**, *51*, 207–210.
34. Nutikka, A.; Binnington-Boyd, B.; Lingwood, C.A. Methods for the purification of Shiga toxin 1. In *Methods in Molecular Medicine*; Philpot, D., Ebel, F., Eds.; Humana Press: Totowa, NY, USA, 2003; pp. 187–195.

35. Nutikka, A.; Binnington-Boyd, B.; Lingwood, C. Methods for the Identification of Host Receptors for Shiga toxin. In *Methods in Molecular Medicine*; Philpot, D., Ebel, F., Eds.; Humana Press: Totowa, NY, USA, 2003; pp. 197–208.
36. Nakajima, H.; Kiyokawa, N.; Katagiri, Y.U.; Taguchi, T.; Suzuki, T.; Sekino, T.; Mimori, K.; Ebata, T.; Saito, M.; Nakao, H.; *et al.* Kinetic analysis of binding between Shiga toxin and receptor glycolipid Gb3Cer by surface plasmon resonance. *J. Biol. Chem.* **2001**, *276*, 42915–42922.
37. Betz, J.; Bielaszewska, M.; Thies, A.; Humpf, H.U.; Dreisewerd, K.; Karch, H.; Kim, K.; Frierich, A.; Muthing, J. Shiga toxin glycosphingolipid receptors in microvascular and macrovascular endothelial cells: association with membrane lipid raft microdomains that differ by their stability to cholesterol depletion. *J. Lipid. Res.* **2011**, *58*, 618–634.
38. Head, S.; Ramotar, K.; Lingwood, C.A. Modification of the glycolipid-binding specificity of vero cytotoxin by Polymyxin B and other cyclic amphipathic peptides. *Infect. Immun.* **1990**, *58*, 1532–1537.
39. Karve, S.S.; Weiss, A.A. Glycolipid binding preferences of Shiga toxin variants. *PLoS One* **2014**, *9*, e101173.
40. Weinstein, D.; Jackson, M.; Holmes, R.; O'Brien, A. Cloning and sequencing of a Shiga-like toxin II variant from an Escherichia coli strain responsible for edema disease of swine. *J. Bacteriol.* **1988**, *170*, 4223–4230.
41. Cummings, M.; Ling, H.; Armstrong, G.; Brunton, J.; Read, R. Modeling the carbohydrate-binding specificity of pig edema toxin. *Biochemistry* **1998**, *37*, 1789–1799.

© 2015 by the authors; licensee MDPI, Basel, Switzerland. This article is an open access article distributed under the terms and conditions of the Creative Commons Attribution license (http://creativecommons.org/licenses/by/4.0/).